Journal of Alloys and Compounds 509 (2011) 2645–2649

Contents lists available at ScienceDirect

Journal of Alloys and Compounds

journal homepage: www.elsevier.com/locate/jallcom

# Room temperature multiferroicity in Bi rich Fe deficient Gd doped $Bi_{1.2}Gd_{0.1}Fe_{0.8}O_3$

S.K. Pradhan[a], J. Das[a], P.P. Rout[a], S.K. Das[a], S. Samantray[a], D.K. Mishra[b], D.R. Sahu[c], A.K. Pradhan[d], K. Zhang[d], V.V. Srinivasu[e], B.K. Roul[a,*]

[a] Institute of Materials Science, Acharya Vihar, Bhubaneswar 751013, India
[b] Institute of Minerals and Materials Technology, Bhubaneswar 751013, India
[c] School of Physics, University of the Witwatersrand, Private Bag-3, Wits 2050, Johannesburg, South Africa
[d] Department of Engineering & Materials Science & Engineering, Norfolk State University, 700 Park Avenue, MVMCAR 523 Norfolk, VA 23504, USA
[e] National Center for Nano Structured Materials, Mechatronics & MicroManufacturing MSM Division Building 14F, Room-131, CSIR, Pretoria, South Africa

ARTICLE INFO

*Article history:*
Received 1 June 2010
Received in revised form
20 November 2010
Accepted 23 November 2010
Available online 30 November 2010

*Keywords:*
Ferroelectric
Solid state reaction
Magnetically ordered materials
X-ray diffraction
Phase transitions

ABSTRACT

A clean signature of room temperature multiferroicity in $Bi_{1.2}Gd_{0.1}Fe_{0.8}O_3$ ceramics is observed. Samples were prepared by slow step sintering technique at 850 °C. Impurity peaks normally present in original $BiFeO_3$ are completely suppressed with the increase of Bi concentration. Apart from this, structural transformation took place from $R3_C$ to $Pn2_1a$ space group and a clear orthorhombic grain growth habit is seen by SEM microstructure. Suppression of impurity phases favors the reduction of mobile oxygen vacancies and hence reduces leakage current for which ferroelectric properties of $Bi_{1.2}Gd_{0.1}Fe_{0.8}O_3$ are enhanced. We argue that the addition of Gd is likely to suppress the spiral spin modulation and at the same time increase the canting angle which favors the enhanced ferromagnetism. Excess Bi is expected to act as point defects and occupy interstitial positions which in turn surrounded by oxygen vacancies and is likely to promote defect driven ferromagnetism with enhanced spin and electric polarization. This finding encourages further revaluation of long-discounted $BiFeO_3$ for multiferroics research.
© 2010 Published by Elsevier B.V.

## 1. Introduction

Recent resurgence of research interest for multiferroic [1–4] materials revived the possibility of strong coupling between the magnetic and ferroelectric order parameters of some promising materials and are likely to be used around room temperature (RT) for possible device design and applications specially in frontier field of spintronic [5] devices, sensor, multiple state memory elements [6], electric field controlled ferromagnetic resonance devices, and transducers with magnetically modulated piezoelectricity [7]. $BiFeO_3$ (BFO) is one of the very few known magnetoelectric system that exhibits antiferromagnetic ordering ($T_N \approx 380$ °C) and ferroelectric behavior with high ferroelectric Curie temperature ($T_C \approx 830$ °C) [8]. It is well documented [9] that due to canting of Fe sub-lattice moment, BFO shows the presence of weak magnetism. It is the primary goal of the researchers over the globe to improve the desired magnetic properties, without altering the ferroelectric properties of the original BFO materials system. To address the issue of enhancing desired magnetic property specially aiming towards ferromagnetic property, a suitable doping in BFO might be the right approach [10–12] to tailor this material in which the linear magneto-electric coupling would exist [13]. It has also been suggested that the spiral spin structure can be changed with the application of a higher magnetic field [14], epitaxial constraint [15] and doping [10]. As far as doping in BFO is concerned, one way of doping is by doping of BFO with rare earth elements [11,12] which are promising to enhance multiferroics properties.

It is well known that gadolinium like lanthanum, belongs to the lanthanides family. The ionic radius of $Gd^{3+}$ (1.11 Å) is close to the ionic radius $Bi^{3+}$ (1.20 Å). Due to same valence of Gd ions with respect to Bi ions, Gd ion doping is expected not to suppress the oxygen vacancies. But suppression of oxygen vacancies is reported to be a cause for the decrease of the leakage current in both bulk and thin film of BFO as seen in case of Ce doped BFO [16]. On the other hand, Gd doping is likely to suppress the impurity phases that are normally appear in BFO and is also reported to be responsible for the reduction of leakage current [17,18] that normally happens due to the suppression of the mobile defects (such as ions of $Fe^{2+}$, vacancies of O and Bi) [19]. It is expected that Gd doping in BFO also suppress spatially modulated spin structure and is likely to increase the canting angle of antiferromagnetically coupled layers due to tilting of $FeO_6$ octahedral [20]. In addition to above, due to the difference in ionic radius, it is also expected that Gd doping

* Corresponding author at: Institute of Materials Science, Planetarium Building, Bhubaneswar 751013, India. Tel.: +91 674 2587649; fax: +91 674 2300142.
*E-mail address:* ims@iopb.res.in (B.K. Roul).

0925-8388/$ – see front matter © 2010 Published by Elsevier B.V.
doi:10.1016/j.jallcom.2010.11.129

could induce structural distortions and may improve the electrical and magnetic properties of Bi rich Fe deficient Gd doped BFO ceramics [21].

Recently, it is reported that crystal structure of Gd-doped BFO sample exhibits the co-existence of orthorhombic and rhombohedral structural phase [22]. In some cases, especially the effect of Gd substitution at Bi site showed a gradual phase transition from rhombohedral to pseudo-tetragonal structure [23] with the increase of Gd contents. Hence, it is evident that doping is very much crucial for structural phase transformation as well as enhancing the multiferroic properties in BFO system. In order to explore the contribution of Gd doping in BFO system for obtaining enhanced ferroelectric and ferromagnetic properties, we have synthesized a series of bismuth rich iron deficient gadolinium doped BFO ceramics and critically optimized its compositional parameter to achieve enhanced multiferroic properties at RT. Although, we have studied different compositions by varying bismuth and iron site, only interesting results pertaining to specific compositions ($BiFeO_3$, $Bi_{1.2}Fe_{0.8}O_3$, $Bi_{0.9}Gd_{0.1}Fe_1O_3$, $Bi_{1.1}Gd_{0.1}Fe_{0.8}O_3$, and $Bi_{1.2}Gd_{0.1}Fe_{0.8}O_3$) are placed in the text for comparison purpose. Primary purpose of considering Bi rich BFO composition is to compensate Bi-loss [24] during sintering at elevated temperature (beyond the melting point of $Bi_2O_3$). This paper reports that at a particular composition ($Bi_{1.2}Gd_{0.1}Fe_{0.8}O_3$), system transforms completely to orthorhombic $Pn2_1a$ polar space group from rhombohedral $R3_C$ symmetry. Both magnetization (M ~ H) and electrical polarization (P ~ E) measurements clearly indicate the co-existence of ferromagnetic and ferroelectric behavior at RT.

## 2. Experimental

Pure BFO, Bi rich Fe deficient BFO, and Gd doped BFO bulk ceramics were synthesized by solid state reaction route. High pure (99.999%) $Bi_2O_3$, $Gd_2O_3$, and $Fe_2O_3$ powders were taken with appropriate composition in an agate mortar. Respective composition of green powders $BiFeO_3$, $Bi_{1.2}Fe_{0.8}O_3$, $Bi_{0.9}Gd_{0.1}Fe_1O_3$, $BiFe_{0.9}Gd_{0.1}O_3$, $Bi_{1.1}Gd_{0.1}Fe_{0.8}O_3$, and $Bi_{1.2}Gd_{0.1}Fe_{0.8}O_3$ was heated at 500 °C for 6 h and then quenched to RT followed by immediate grinding. Similar procedure was repeated for five times in order to achieve homogeneous mixture of green powders with smaller particle size. Green powders of respective composition were pelletized using freshly prepared poly vinyl alcohol as binder. Cylindrical pellets having dimension 13 mm diameter and 2 mm thickness were prepared by using hydraulic press with a pressure of 10 ton/cm$^2$. Pressed pellets were slowly heated (50 °C/h) to 600 °C and kept for 8 h to release PVA binder from pellets using high temperature programmable (Eurotherm controller, Model: 2204) vacuum furnace. Pellets were sintered by slow step sintering schedule at 850 °C for 24 h and characterized by XRD, SEM, magnetization and electrical polarization.

X-ray diffraction (XRD) pattern of the samples was carried out in the $2\theta$ range (20–80°) using Cu $K_\alpha$ radiation by a Philips diffractometer (Model 1715) fitted with monochromator and operated at 40 kV and 20 mA. The ferroelectric (electric polarization as a function of electric field) measurements of sintered pellets were carried out by using ferroelectric hysteresis loop tracer precession LC from Radiant technology, USA. Magnetization measurements of sintered samples were carried out by using SQUID Magnetometer (Quantum Design-MPMS) with maximum field of one tesla. All hysteresis measurements of the samples were taken at room temperature.

## 3. Results and discussion

Fig. 1 shows the XRD pattern of $BiFeO_3$, $Bi_{1.2}Fe_{0.8}O_3$, and $Bi_{1.2}Gd_{0.1}Fe_{0.8}O_3$ ceramics sintered at 850 °C for 24 h. Respective peaks in XRD pattern are indexed (Fig. 1(a)–(c)) with $h\,k\,l$ indices using search test programme [25]. XRD peaks of pure BFO are fitted to $R3_C$ space group having lattice parameters $a = 5.590$ Å, and $c = 13.880$ Å. However, there are some more $h\,k\,l$ reflections present in the XRD pattern of Fig. 1(a) which corresponding to impurity phases belonging to high order bismuth and iron rich oxide phases such as $Bi_{25}FeO_{40}$, and $Bi_2Fe_4O_9$. These peaks are normally found in BFO system [26,27]. It is evident that the deficient of bismuth in the original BFO system are likely to be the principal factor to exhibit above impurity phases. XRD pattern of a typical Bi rich BFO ($Bi_{1.2}Fe_{0.8}O_3$) is shown in Fig. 1(b). It is noted that the impurity phases that are observed in Fig. 1(a) completely suppressed in $Bi_{1.2}Fe_{0.8}O_3$. Apart from impurity phases, both samples showed normal peak splitting in XRD pattern that appear within 31–33°, 38.5–40.5°, 51–52°, and 57–58° of $2\theta$ values [28,29]. It is inferred from Fig. 1(b) that Bi rich iron deficient BFO samples exhibit near monophasic $R3_C$ symmetry.

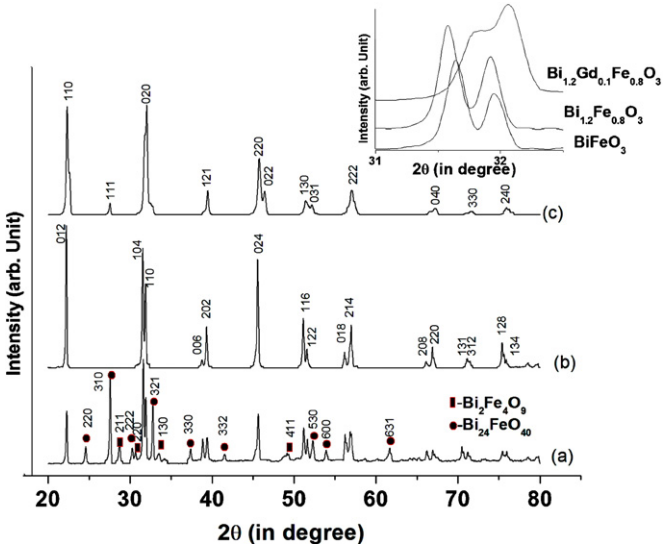


**Fig. 1.** XRD patterns of (a) $BiFeO_3$, (b) $Bi_{1.2}Fe_{0.8}O_3$, and and (c) $Bi_{1.2}Gd_{0.1}Fe_{0.8}O_3$ pellets sintered at 850 °C for 24 h using slow step sintering schedule (50 °C/h). Inset figure shows magnified pattern of above samples in the vicinity of of $2\theta = 31$–$32°$.

In order to understand the role of Gd doping in BFO system, we have carried out XRD studies of Bi rich Gd doped BFO system of bulk ceramics sintered at 850 °C for 24 h. Magnified pattern of pure BFO, Bi rich BFO, and Bi rich Fe deficient Gd doped BFO in the vicinity of $2\theta = 32°$ are shown in inset of Fig. 1 which showed that diffraction peaks (1 0 4 and 1 1 0) are clearly separated in pure BFO and Bi rich BFO. But XRD peaks are shifted and overlapped to a single broad peak in case of Bi rich Fe deficient Gd doped BFO. Further analysis revealed that XRD peak at $2\theta = 38.85°$ is assigned to (0 0 6) $h\,k\,l$ value for the rhombohedral structure of pure BFO and Bi rich BFO. This peak become weak and disappears when Gd atoms are substituted ($Bi_{1.2}Gd_{0.1}Fe_{0.8}O_3$). Disappearance of (0 0 6) peak indicates the structural transformation from rhombohedral phase to orthorhombic phase [18]. Fig. 1(c) shows the XRD pattern of $Bi_{1.2}Fe_{0.8}Gd_{0.1}O$ sintered ceramics. It is very much interesting to observe that highly intense and sharp XRD peaks of Bi rich Fe deficient Gd doped BFO (GBFO) were indexed with $h\,k\,l$ indices and fitted to either orthorhombic $Pnma$ or $Pn2_1a$ space groups with similar lattice parameter ($a = 5.579$ Å, $b = 7.94$ Å, and $c = 5.440$ Å). It is further important to note here that even though the material is polycrystalline in character, the crystalline peaks at lower $2\theta$ values are very prominent and intense. The reflection conditions derived from the indexing of our observed diffraction pattern were found to be compatible with the space groups mentioned above [30]. However, orthorhombic $Pnma$ structure is non-polar in nature and $Pn2_1a$ space group allows polar displacements along $b$-axis [22]. As we have observed clean ferroelectric loops (to be discussed later), we confirmed that $Pn2_1a$ is non-centrosymmetric orthorhombic space group for $Bi_{1.2}Fe_{0.8}Gd_{0.1}O$ sintered ceramic.

Microstructure analysis of Bi rich Fe deficient Gd doped BFO are carried out by SEM and shown in Fig. 2(a) and (b). From the SEM photographs, it is clearly visible that identical grains with a particular growth habit are closely packed without presence of any auxiliary grain growth habit as seen from Fig. 2(a). Densely packed orthorhombic crystallites of different dimensions are almost homo-

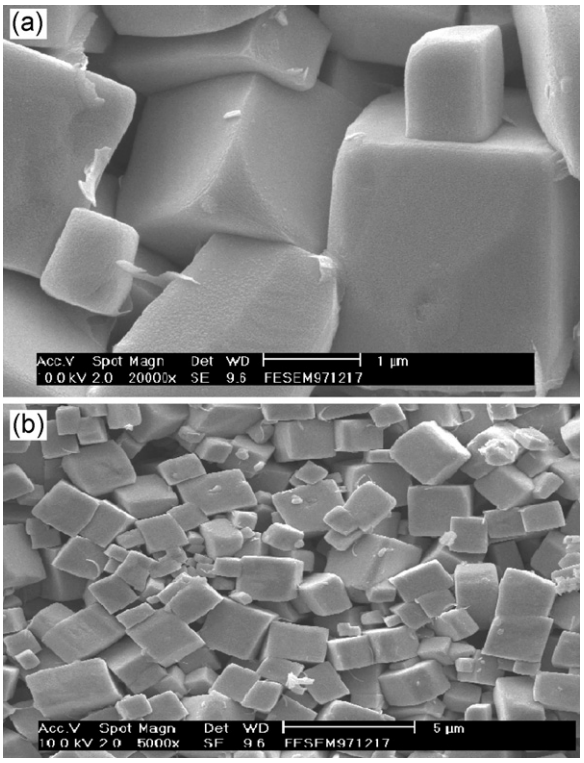


**Fig. 2.** SEM image of $Bi_{1.2}Gd_{0.1}Fe_{0.8}O_3$ Bi rich Fe deficient Gd doped bulk BFO sintered by slow step sintering schedule.

geneously distributed leaving relatively less scope for development of uneven and irregular pore structure inside the bulk. It is also equally very important to note that almost all microcrystallites are identical with orthorhombic grain growth habit as shown in Fig. 2(b).

In order to understand the role of bismuth, we have prepared and studied bismuth deficient Fe rich Gd doped BFO ($Bi_{0.9}Gd_{0.1}Fe_1O_3$), and Bi rich Fe deficient Gd doped BFO ($Bi_1Gd_{0.1}Fe_{0.9}O_3$, $Bi_{1.1}Gd_{0.1}Fe_{0.8}O_3$, and $Bi_{1.2}Gd_{0.1}Fe_{0.8}O$). $M \sim H$ behavior of above sintered specimen were carried out at room temperature which are shown in Fig. 3(a)–(d). It is clearly observed from Fig. 3(a) that Bi deficient Gd-doped BFO ceramics ($Bi_{0.9}Gd_{0.1}Fe_1O_3$) did not show any observable ferromagnetic loop even if magnetic field sweeps up to 8000 Oe at RT. However, when appropriate bismuth ion ($Bi_1Gd_{0.1}Fe_{0.9}O_3$) is maintained in BFO materials with same level of Gd doping, a weak but observable ferromagnetic state is observed at RT which is further enhanced to a clear ferromagnetic loop without saturation when excess Bi is further added into Gd-doped BFO ($Bi_{1.1}Gd_{0.1}Fe_{0.8}O_3$ and $Bi_{1.2}Gd_{0.1}Fe_{0.8}O_3$) bulk ceramics as shown in Fig. 3(c) and (d).

Although the origin of ferromagnetic states is still not clear and a question under debate, but some experimental observation [31] as well as theoretical analysis [32] inferred that suppression of helical order with periodicity about 620 Å on canted antiferromagnetic order between two successive (1 1 1) ferromagnetic planes, might give rise to higher magnetization. Secondly, substituent in BFO system can further destroy spiral modulated spin structure and hence showed enhanced magnetization [32]. Enhanced ferromagnetic behavior has already been shown by the substitution of transition metal ions (Mn) at Fe site [33] as well as rare earth (La) at Bi site [34] in multiferroic BFO system. As explained by other researchers, spiral G-type antiferromagnetic spin structure of un-doped BFO shifts towards a collinear G-type antiferromagnetic structure with increasing Mn concentration [32] as a result of which suppression of spiral spin structure takes place resulting the enhance macroscopic magnetization by the canted spin structure[32]. Our present observation of enhanced ferromagnetism in Bi rich Fe deficient Gd doped BFO clearly supports the idea of suppression of spiral modulated spin structure.

On the other hand, it was observed that epitaxial strain and oxygen vacancies associated with $Fe^{2+}$ ions contribute to the magnetization [35,36]. Here, the contribution of the size effect has no role in exhibiting the weak ferromagnetic order in bulk sintered BFO. Only point defect caused by the doping of Gd and excess of Bi ion occupying interstitial position are likely to be responsible for exhibiting enhanced ferromagnetic order in sintered Bi rich Fe deficient Gd doped BFO bulk ceramic. It is noted that a prominent $M \sim H$ loop with remanent magnetization at about 0.04 emu/gm is associated as shown in Fig. 3(d). Our observations clearly indicate that increases of Bi with Fe deficient are definitely contributing to enhanced ferromagnetic behavior at RT. Now the basic question arises regarding the role of excess Bi in Fe deficient Gd doped BFO system in connection with exhibiting enhanced ferromagnetism at RT. As such, Bi is known to be non-magnetic and deficient of Fe in BFO is detrimental for exhibiting ferromagnetism. On the other hand, keeping Gd concentration fixed (0.1) why Bi rich BFO showed enhanced ferromagnetism? To address the issue, we concentrate on the role of nonmagnetic Bi ion as the cause for enhancing ferromagnetic signature. Excess bismuth in this BFO system may act as a point defect and occupied in interstitials. When this interstitial Bi position surrounded by oxygen vacancies (more than one preferably) probably, ferromagnetism is induced in the system as observed in case of Zn (non-magnetic) surrounded by oxygen vacancies [37]. Further detail explanation to this effect is highly essential so that BFO can be tailored to achieve desired properties for real multiferroics device applications.

Apart from the reasons mentioned above to explain ferromagnetism observed in $Bi_{1.2}Gd_{0.1}Fe_{0.8}O_3$, followings are the two possible reasons for enhance magnetization come from the bulk sintered ceramics of $Bi_{1.2}Gd_{0.1}Fe_{0.8}O_3$. In a typical situation, presence of transition element (like Fe in present case) when it is either dissolved in or residing on the surface of certain metal oxides matrix [38], it gives rise to unusual large magnetic moment which is believed to be originated from ferromagnetic coupling mediated by electrons [38,39]. In our present case, we argued that due to large difference of ionic radius of $Fe^{3+}$ (0.67 Å) with respect to $Bi^{3+}$ (1.20 Å) and $Gd^{3+}$ (1.11 Å), it is possible for Fe to be either dissolved or reside on the surface even if the primary composition is Fe deficient. Another possible cause for observing enhanced magnetism in present $Bi_{1.2}Gd_{0.1}Fe_{0.8}O_3$ may be due to the presence of Gd which may be explained in terms of a long range spin polarization as observed in case of Gd in GaN [40]. However, exact cause for enhanced magnetism in present composition is still a matter of debate and more experimental evidences are required.

As per our experimental observation, excess bismuth in BFO ($Bi_{1.2}Gd_{0.1}Fe_{0.8}O_3$) promotes ferromagnetism as compared to the $BiFeO_3$ bulk ceramics sintered at 850 °C for 24 h using slow step sintering schedule. In order to understand the contribution of real rate of $Bi^{3+}$ ions in bismuth rich $Bi_{1.2}Gd_{0.1}Fe_{0.8}O_3$ sample sintered at 850 °C, we have analyzed our magnetization ($M \sim H$) data for different magnetic fields. As the real rate of $Bi^{3+}$ ions in Bi rich $Bi_{1.2}Gd_{0.1}Fe_{0.8}O_3$ is proportional to the excess of bismuth metal ions concentration incorporated during materials processing stage, it would be appropriate to present and analyze the data for the contribution of excess bismuth in $Bi_{1.2}Gd_{0.1}Fe_{0.8}O_3$ for enhanced magnetization. Fig. 4 shows the magnetization value as a function of bismuth concentration at a field of 5000 Oe. It is observed that keeping other metal ions (Gd and Fe) fixed, excess bismuth ($Bi_{1.2}$) promotes huge saturation magnetization value (0.08 emu/gm) with respect to ($Bi_{1.0}$) magnetization value (0.000085 emu/g). It is esti-

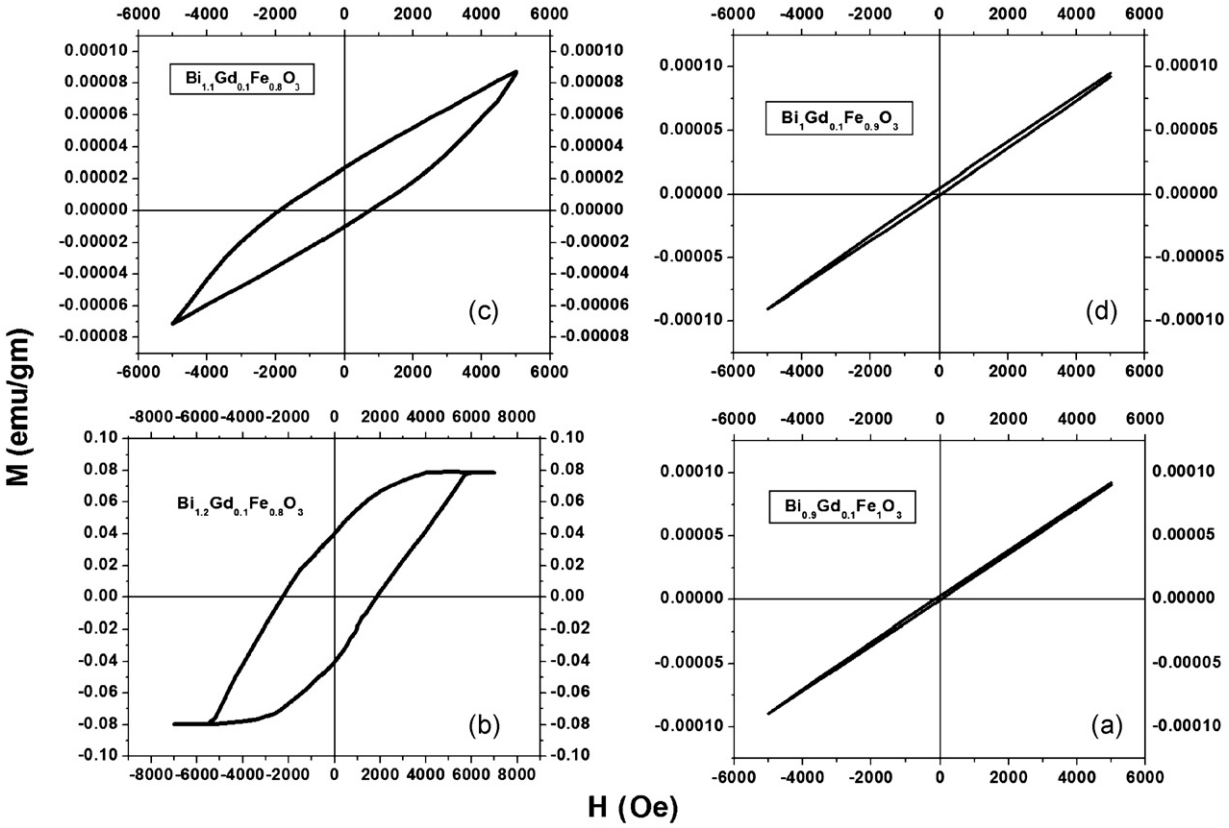


**Fig. 3.** Room temperature M–H hysteresis loops of (a) $Bi_{0.9}Gd_{0.1}Fe_1O_3$ (b) $BiFe_{0.9}Gd_{0.1}O_3$ (c) $Bi_{1.1}Gd_{0.1}Fe_{0.8}O_3$, and (d) $Bi_{1.2}Gd_{0.1}Fe_{0.8}O_3$ samples sintered at 850 °C for 24 h using slow step sintering schedule.

mated that there are $8.618 \times 10^{20}$ excess of $Bi^{3+}$ ions present in $Bi_{1.2}Gd_{0.1}Fe_{0.8}O_3$ sample sintered at 850 °C as $Bi^{3+}$ in $Bi_2O_3$.

It is well established [14,41] that crystal structure of the polar phase of BFO is described by the rhombohedral $R3_C$ space group. This symmetry allows antiphase octahedral tilting and ionic displacements from the centro symmetric hexagonal setting position along $[0\,0\,1]_H$ direction and permits the existence of weak ferromagnetic moment originating from Dzyaloshinsky–Moriya interaction [11]. However, a cycloid type spatial spin modulation superimposed to the G-type antiferromagnetic spin ordering [14], prevents the observation of any net magnetization and linear magnetic effects [42]. As known, pure BFO exhibits a linear magnetic field dependence of magnetization of typical antiferromagnetic

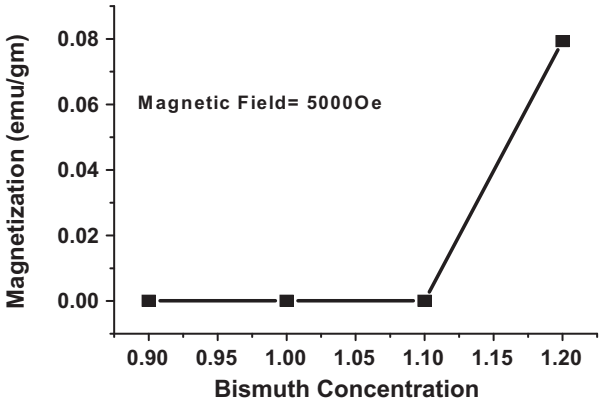


**Fig. 4.** Magnetization as a function of bismuth concentration for samples $Bi_{0.9}Gd_{0.1}Fe_1O_3$, $BiFe_{0.9}Gd_{0.1}O_3$, $Bi_{1.1}Gd_{0.1}Fe_{0.8}O_3$, and and $Bi_{1.2}Gd_{0.1}Fe_{0.8}O_3$ at a field of 5000 Oe at room temperature.

nature. However, in case of our Gd doped BFO ($Bi_{1.2}Gd_{0.1}Fe_{0.8}O_3$), we observe clear signature of ferromagnetic behavior in Fig. 3(d). Present observation of net magnetization in Gd-doped BFO (Gd-BFO) may be related to an anti-symmetric exchange mechanism [43,44] and substitution induced suppression of spiral spin modulation [42] which may be its prime cause. Without suppression of spiral spin modulation in iron sublattice, Gd magnetic moment cannot contribute to nonzero remanent magnetization and significant coercivity as observed in our present Gd-BFO system even though $Gd^{3+}$ ions are magnetically active. Hence, we infer that Gd substitution definitely suppresses the spiral spin modulation and inturn favors the ferromagnetism in Gd-BFO.

In order to ascertain the ferroelectric behavior of Gd doped BFO, polarization as a function of electric field, measurements were carried out at room temperature using ferroelectric loop tracer set-up which are shown in Fig. 5(a)–(c). Fig. 5(a) shows the polarization vs. electric field behavior of $BiFe_{0.9}Gd_{0.1}O_3$ with saturation polarization of 11 $\mu C/cm^2$. With the increasing concentration of Bi in Gd doped BFO ($Bi_{1.1}Gd_{0.1}Fe_{0.8}O_3$), the saturation polarization ($P$) value increases to 13 $\mu C/cm^2$ which is shown in Fig. 5(b) at room temperature. It is clearly evident from Fig. 5(c) that Bi-rich ($Bi_{1.2}Gd_{0.1}Fe_{0.8}O_3$) samples showed enhanced P ~ E loop with larger surface area contributing enhanced saturation polarization value (13–15 $\mu C/cm^2$) with respect to $Bi_{1.1}Gd_{0.1}Fe_{0.8}O_3$. Pure BFO bulk always showed low polarization value (≈9 $\mu C/cm^2$) [45] which is detrimental for any device application. Our present result of Bi rich Fe deficient Gd doped BFO ($Bi_{1.2}Gd_{0.1}Fe_{0.8}O_3$) clearly overcomes this problem and at RT, Gd doped BFO showed enhanced saturation polarization value.

As known, due to uncertain oxygen stochiometry, low resistivity, high defect concentration and poor sample (inhomogeneous bulk sample structure) quality, BFO has been expected to lose

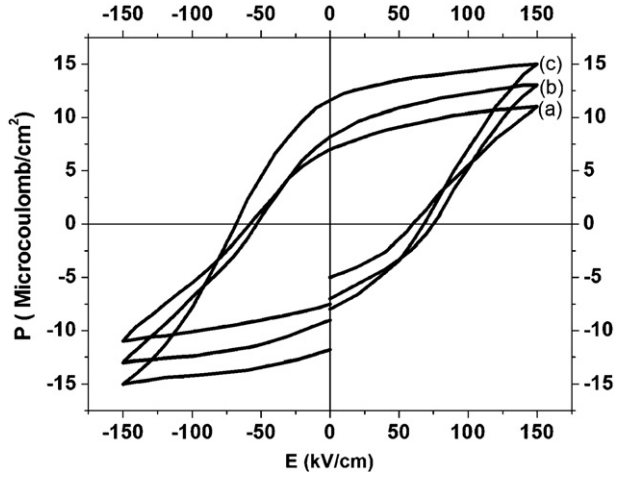


**Fig. 5.** Room temperature P–E hysteresis loops of (a) $BiGd_{0.1}FeO_3$, (b) $Bi_{1.1}Gd_{0.1}Fe_{0.8}O_3$, and (c) $Bi_{1.2}Gd_{0.1}Fe_{0.8}O_3$ samples sintered at 850 °C for 24 h using slow step sintering schedule.

its commercial viability ground although it was discussed almost before five decades. Low resistivity associated with this system known to be hindered the moment of ferroelectric domains under external applied electric field and prevent the ferroelectric hysteresis character, which is the fundamental requirement for practical application in memory devices and other related multiferroics applications. Our present preparation method including the selection of metal ions as substituent in BFO ceramics certainly eliminates some of the negative issues and exhibit that BFO bulk ceramics can be tailored to be an impurity phase free BFO materials system to achieve enhanced multiferroics properties.

## 4. Conclusion

In summary, we conclude that Bi rich Fe deficient Gd doped BFO multiferroics ceramics can be prepared by our novel slow step sintering method. Original BFO structure completely changed from rhombohedral $R3_C$ symmetry to monophasic orthorhombic ($Pn2_1a$) without appearance of any secondary phases and showed a clear signature of enhanced multiferroics behavior. Co-existence of room temperature ferromagnetic and ferroelectric behavior is confirmed from magnetization and polarization measurements which clearly exhibit enhanced multiferroics behavior. SEM microstructure also showed clear and sharp orthorhombic grain growth habit. We emphasized that excess bismuth is expected to act as point defects and occupy in interstitials which in turns surrounded by oxygen vacancies. These defects are likely to promote defect driven ferromagnetism in BFO system [34]. Incorporation of Gd in the presence of excess bismuth in BFO enhanced both spin and electric polarization at room temperature. We also infer that Gd substitution in BFO probably suppresses the spiral spin modulation and inturn favors the ferromagnetism in Gd-BFO [14]. Our present findings definitely encourage further research interest and motivation of the long discounted $BiFeO_3$, especially with regard to its promising utility in multiferroics memory devices.

## Acknowledgement

Authors Sangram Keshari Pradhan and Prajna Priyadarshinee Rout are gratefully acknowledged the financial support and research facilities received from Institute of Materials Science.

## References

[1] Q.H. Jiang, F.T. Liu, C.-W. Nan, Y.-H. Lin, M.J. Reece, H.X. Yan, H.P. Ning, Z.J. Shen, Appl. Phys. Lett. 95 (2009) 012909.
[2] S. Hunpratub, P. Thongbai, T. Yamwong, R. Yimnirun, S. Maensiri, Appl. Phys. Lett. 94 (2009) 062904.
[3] X.-Y. Zhang, Q. Song, F. Xu, C.K. Ong, Appl. Phys. Lett. 94 (2009) 022907.
[4] A. Lahmar, S. Habouti, M. Dietze, C.-H. Solterbeck, M. Es-Souni, Appl. Phys. Lett. 94 (2009) 012903.
[5] J. Wang, J.B. Neaton, H. Zheng, V. Nagarajan, S.B. Ogale, B. Liu, D. Viehland, V. Vaithyanathan, D.G. Schlom, U.V. Waghmare, N.A. Spaldin, K.M. Rabe, M. Wuttig, R. Ramesh, Science 299 (2003) 1719.
[6] Y. Wang, C.W. Nan, Appl. Phys. Lett. 89 (2006) 052903.
[7] N.A. Hill, J. Phys. Chem. B 104 (2000) 6694.
[8] W. Eerenstein, N.D. Mathur, J.F. Scott, Nature (London) 442 (2006) 759.
[9] G.A. Smolenskii, L. Chupis, Sov. Phys. USP 25 (1982) 475.
[10] F. Bai, J. Wang, M. Wutting, J.F. Li, N. Wang, A. Pyatakov, A.K. Zvezdin, L.E. Cross, D. Viehland, Appl. Phys. Lett. 86 (2005) 032511.
[11] C. Ederer, N.A. Spaldin, Phys. Rev. B 71 (2005) 060401.
[12] D. Lee, M.G. Kim, S. Ryu, H.M. Jang, S.G. Lee, Appl. Phys. Lett. 86 (2005) 222903.
[13] A. Singh, V. Pandey, R.K. Kotnala, D. Pandey, Phys. Rev. Lett. 101 (2008) 247602.
[14] I. Sosnowska, T. Peterlin-Neumaier, E. Steichele, J. Phys. C 115 (1982) 4835.
[15] S.W. Cheong, M. Mostovoy, Nat. Mater. 6 (2007) 13.
[16] J. Liu, M. Li, L. Pei, J. Wang, B. Yu, X. Wang, X. Zhao, J. Alloy Compd. 493 (2010) 544.
[17] V.R. Palkar, D.C. Kundaliya, S.K. Malik, S. Bhattacharya, Phys. Rev. B 69 (2004) 212102.
[18] S.-T. Zhang, Y. Zhang, M. Liu, C. Du, Y. Chen, Z. Liu, Y. Zhu, N.-B. Ming, Appl. Phys. Lett. 88 (2006) 162901.
[19] G.L. Yuan, S.W. Or, Y.P. Wang, Z.G. Liu, J.M. Liu, Solid State Commun. 138 (2006) 76.
[20] V.B. Naik, R. Mahendiran, Solid State Commun. 149 (2009) 754.
[21] M. Al-Haj, Cryst. Res. Technol. 45 (2010) 89.
[22] V.A. Khomchenko, V.V. Shvartsman, P. Borisov, W. Kleemann, D.A. Kiselev, I.K. Bdikin, J.M. Vieira, A.L. Kholkin, J. Phys. D: Appl. Phys. 42 (2009) 045418.
[23] G.D. Hu, X. Cheng, W.B. Wu, C.H. Yang, Appl. Phys. Lett. 91 (2007) 232909.
[24] A.Z. Simoes, F.G. Garcia, C.S. Riccardi, Mater. Chem. Phys. 116 (2009) 305.
[25] B.K. Roul, J. Supercond. 14 (4) (2001) 529.
[26] J.K. Kim, S.S. Kim, W.J. Kim, Mater. Lett. 59 (2005) 4006.
[27] R. Majumdar, P.S. Devi, D. Bhattacharya, P. Choudhury, A. Sen, Appl. Phys. Lett. 91 (2007) 062510.
[28] L.Y. Wang, D.H. Wang, H.B. Huang, Z.D. Han, Q.Q. Cao, B.X. Gu, Y.W. Du, J. Alloys compd. 469 (2009) 1–3.
[29] Z.X. Cheng, A.H. Li, X.L. Wang, S.X. Dou, K. Ozawa, H. Kimura, S.J. Zhang, T.R. Shrout, J. Appl. Phys. 103 (2008) 07E507.
[30] T. Hahn (Ed.), International Tables for Crystallography, vol. A, Kluwer, Dordrecht, 2002.
[31] X. Yu, X. An, Solid State Commun. 149 (2009) 711.
[32] J.P. Tae, C. Georgia, Nano Lett. 7 (2007) 766.
[33] I. Sosnowska, N.T. Peterlin, E. Steichele, J. Phys. C: Solid State Phys. 15 (1982) 4835.
[34] Z.X. Cheng, X.L. Wang, S.X. Dou, Phys. Rev. B 77 (2008) 092101.
[35] W. Eerenstein, F.D. Marrison, J. Dho, M.G. Blamire, J.F. Scott, N.D. Mathur, Science 307 (2005) 1203a.
[36] J.B. Li, G.K. Rao, J.K. Liang, Y.K. Liu, J. Luo, J.R. Chen, Appl. Phys. Lett. 90 (2007) 162513.
[37] S. Banerjee, M. Mandal, N. Gayathri, M. Sardar, Appl. Phys. Lett. 91 (2007) 182501.
[38] G. Bergmann, Phys. Rev. B 23 (1981) 3805.
[39] J.M.D. Coey, et al., Appl. Phys. Lett. 84 (2004) 1332.
[40] S. Dhar, O. Brandt, M. Ramsteiner, V.F. Sapega, K.H. Ploog, Phys. Rev. Lett. 94 (2005) 037205.
[41] C. Michel, J.M. Moreau, G.D. Achenbach, R. Gerson, W.J. James, Solid State Commun. 7 (1969) 701.
[42] I. Dzyaloshinsky, J. Phys. Chem. Solids 4 (1958) 241.
[43] T. Moriya, Phys. Rev. 120 (1960) 91.
[44] A.M. Kadomtseva, Yu.F. Popov, A.P. Pyatakov, G.P. Vorob'ev, A.K. Zvezdin, D. Viehland, Phase Transit. 79 (2006) 1019.
[45] Y.P. Wang, G.L. Yuan, X.Y. Chen, J.-M. Liu, Z.G. Liu, J. Phys. D 39 (2006) 2019.